



Hydrogeochemical characteristics and groundwater quality assessment in the plain area of Yarkant River Basin in Xinjiang, P.R. China

Jie Zhang^{1,2} · Jinlong Zhou^{1,2} · Yinzhu Zhou³ · Yanyan Zeng^{1,2} · Yuanyuan Ji^{1,2} · Ying Sun^{1,2} · Mi Lei^{1,2}

Received: 6 October 2020 / Accepted: 3 February 2021 / Published online: 20 February 2021
© The Author(s), under exclusive licence to Springer-Verlag GmbH, DE part of Springer Nature 2021

Abstract

The deteriorating groundwater quality due to natural genesis and anthropogenic activities has prevented the sustainable use of groundwater. The characteristics and factors affecting groundwater quality for drinking in shallow aquifers (depth ≤ 100 m) in the plain area of Yarkant River Basin in Xinjiang were analyzed using water quality index (WQI), geostatistics, and geochemical methods. Results showed that the groundwater was weak-alkaline with neutral pH, with dominant water types being $\text{SO}_4\cdot\text{HCO}_3\text{-Ca}\cdot\text{Mg}$, $\text{SO}_4\cdot\text{Cl}\cdot\text{HCO}_3\text{-Na}\cdot\text{Ca}$, $\text{SO}_4\cdot\text{HCO}_3\cdot\text{Cl}\text{-Ca}\cdot\text{Na}$, $\text{Cl}\cdot\text{SO}_4\text{-Na}\cdot\text{Ca}$, and $\text{HCO}_3\cdot\text{SO}_4\text{-Mg}\cdot\text{Ca}$. WQI ranged between 31.79 and 549.37, and about 14.43%, 31.96%, 18.56%, 22.68%, and 12.37% of the all samples were excellent, good, medium, poor, and extremely poor quality, respectively. The proportion of excellent quality was the highest in single structure phreatic aquifer (SSPA, 50.00%) and good quality were the highest in multilayered structure phreatic aquifer (MSPA, 34.21%) and multilayered structure confined aquifer (MSCA, 28.89%). With the extension of the river, the groundwater quality gradually degenerated from south to north in phreatic aquifer (PA, including SSPA and MSPA). The further away from the Yarkant river, the worse the groundwater quality of PA. Furthermore, the WQI showed excellent, good, and an alternation of medium and poor quality (including extremely poor quality) from south to north in the MSCA. The groundwater quality deterioration might have been affected by the dissolution of evaporite minerals, such as halite, gypsum, and anhydrite and ion exchange process. In addition, local effects of anthropogenic activities and land usage patterns on the groundwater quality should be reckoned as well.

Keywords Hydrogeochemical characteristics · Water quality index · Entropy weight · Geostatistics · Saturation index · Yarkant River Basin

Introduction

Groundwater, especially in arid and semi-arid regions, has become the most important water source for drinking,

irrigation, industry, and all other sectors (Kolsi et al. 2013; Singh et al. 2010; Solangi et al. 2019). Many areas in Central Asian, such as Iran (Dehbandi et al. 2018; Keshavarzi et al. 2011), Pakistan (Naseem et al. 2018; Solangi et al. 2019; Tabassum et al. 2019), Afghanistan (Ali et al. 2020; Hayat and Baba 2017), and northwest China (Huang and Pang 2012; Li et al. 2013; Lin et al. 2018) have been affected by degraded of groundwater quality, which has been preventing regional economic development. The quality of groundwater is deteriorating by the natural processes (e.g., evapotranspiration, mineral dissolution and recharge water quality) and anthropogenic activities (e.g., agricultural irrigation input, infiltration of domestic sewage and industrial wastewater and change of land-use and land-cover patterns) (Bhakar and Singh 2018; Bouzourra et al. 2015; Schwarzenbach et al. 2010). Groundwater quality of confined aquifer in the Yinchuan region, northwest China, was controlled mainly by the dissolution of minerals, mixing between

Responsible Editor: Xianliang Yi

✉ Jinlong Zhou
zjzhoujl@163.com

✉ Yinzhu Zhou
yinzhu_zhou@qq.com

¹ College of Water Conservancy and Civil Engineering, Xinjiang Agricultural University, Urumqi 830052, China

² Xinjiang Hydrology and Water Resources Engineering Research Center, Urumqi, China

³ Center for Hydrogeology and Environmental Geology, China Geological Survey, Baoding 071051, China

the confined groundwater and polluted unconfined groundwater, and effects of ion exchange (Zhang et al. 2016). In addition, over-abstraction of groundwater for agricultural irrigation was causing the depletion and deterioration of aquifers around the world, and over-fertilizer was also degraded water quality (Pulido-Bosch et al. 2018). Therefore, the groundwater scientists have focused on assessing groundwater quality and its suitability for drinking, domestic, irrigation, and industrial uses (Adimalla et al. 2020; Bouteraa et al. 2019; Islam et al. 2017a, 2020b; Saha et al. 2020).

Groundwater quality evaluation is essential for managed groundwater development (Egbi et al. 2018). Water quality index (WQI) is an effective method to assess groundwater quality (Bouteraa et al. 2019; Rabeiy 2018; Solangi et al. 2019). The WQI integrated each parameter as well as many qualitative parameters into a single value using the drinking water quality standards proposed by the WHO (2011). A weight of each groundwater quality parameter was assigned according to their significance in the overall water quality. Based on their practical experience, many researchers (Alghamdi et al. 2020; Bhuiyan et al. 2016; Islam et al. 2020b; Reyes-Toscano et al. 2020; Sethy et al. 2017) assigned a weight between 1 and 5 to each indicator, which was used in calculating the relative weight using weighted arithmetic index method. However, weights were determined by experts' experience might lead to over- or under-emphasizing some parameters, thus affecting the results (Maskooni et al. 2020). To reduce the errors while subjectively selecting the weights, WQI based on entropy weight (Adimalla et al. 2020; Islam et al. 2017a, 2020a; Maskooni et al. 2020) was applied for assessing the groundwater quality in the plain area of the Yarkant River Basin in Xinjiang, China.

The plain area of the Yarkant River Basin has an irrigated area of approximately 500,000 hm², the largest irrigated areas in Xinjiang, northwest China. Groundwater is the main water source for agricultural and domestic purposes in the Yarkant River Basin. With rapid economic development, deteriorating groundwater quality has become a major constraint to sustainable socio-economic development and environmental protection in the region (Luan et al. 2017). It was very essential to deeply understand the factors influencing groundwater quality and its spatial variability for decision-making in any particular region (Islam et al. 2017a). However, the research on the assessment of groundwater quality for drinking purposes in the Yarkant River Basin was very limited. The characterization of groundwater quality and its spatial variation in the Yarkant River Basin using comprehensive evaluation and geostatistical approaches were yet to be conducted. In this study, WQI, statistics, geostatistics, ionic ratios, and geochemical equilibrium modelling were used to assess the groundwater quality for drinking purposes and analyze the spatial distribution characteristics and its factors of groundwater quality in this region.

Materials and methods

Study area

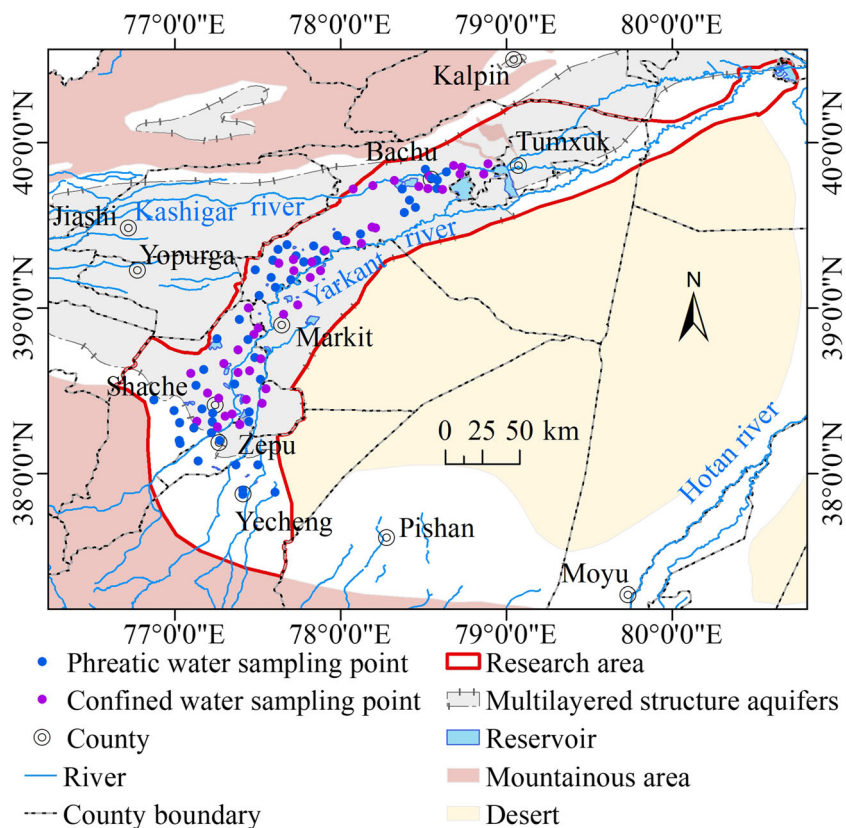
The Yarkant River Basin is located in the southern part of Xinjiang, northwest China, and can be divided into two units: southern mountainous and northern plain areas. The plain area (37° 22' to 40° 29' N, 76° 38' to 80° 45' E) is located in the middle of northern piedmont of the Kunlun Mountains, with Jiashi and Yopurga counties in the Kashi Prefecture and Taklimakan Desert situated in the west and east, respectively. The study area is shown in Fig. 1. The plain area of the Yarkant River Basin is a typical dry continental climate (Chang et al. 2016). The average annual temperature is 11.9 °C, annual precipitation is 52.7 mm, and annual potential evaporation is 2454 mm in this area.

The hydrogeological conditions of the study area are shown in Fig. 2. Groundwater recharge is mainly produced from the seepage of rivers and reservoirs, and irrigation water infiltration through permeable exposures (Zhang et al. 2019). Groundwater flows mainly along rivers from south to north. Evaporation and transpiration, spring drainage, and pumping are the main groundwater outputs. Piedmont plain area is mainly distributed in the north of Yecheng to Shache county, which is a single structure phreatic aquifer (SSPA). This area has good permeability and water conductivity, large hydraulic gradient, and smooth groundwater runoff, with highly thick medium coarse, medium fine, and fine sands (Kang et al. 2016). Alluvial plain is located in the middle of the study area, including Markit county and Bachu county, and the aquifer is mainly composed of multilayered structure phreatic and confined aquifers. This area has poor permeability and water conductivity, gentle hydraulic slope, and slow groundwater runoff (Wu et al. 2008). Clay layers situated in the middle of the study area are usually found at the depths of approximately 10 to 20 m below the land surface and separate the above multilayered structure phreatic aquifer (MSPA) from below multilayered structure confined aquifer (MSCA). Deposits in the confined aquifer consist of a sequence of fine, silty, and clayey sands up to 20 m thick, consisting of a fine-grained silty-clayey matrix.

Sample collection and analysis

In August–September 2018, 97 shallow groundwater samples (at the sampling depths of less than 100m) were collected from the study area (Fig. 1), including 14 from SSPA, 38 from MSPA, and 45 from MSCA. The total dissolved solids (TDS), total hardness (TH), dissolved oxygen (DO), pH, K⁺, Na⁺, Ca²⁺, Mg²⁺, Cl⁻, SO₄²⁻, HCO₃⁻, NO₃⁻, and F⁻ concentrations were measured at the water quality laboratory of the NO.2 Hydrogeological and Engineering Geological Team of Xinjiang Bureau of Geology and Mineral Resources

Fig. 1 Location map of groundwater sampling points situated in the study area



Exploration and Development. Concentrations of K^+ and Na^+ were determined using flame atomic absorption spectrophotometry. TH , Ca^{2+} , Mg^{2+} , and HCO_3^- concentrations were determined using ethylenediamine disodium tetraacetic acid titration method. TDS , Cl^- , SO_4^{2-} , NO_3^- and F^- concentrations were measured by 105 °C drying-gravimetric method, silver nitrate volumetric method, barium sulfate turbidimetry, spectrophotometric method, and ion-selective electrodes method (PHS-3D), respectively. Concentrations of NO_3^- and other chemical constituents mentioned above were determined with the detection limits of 0.05 and 0.01 $mg \cdot L^{-1}$. For all samples, the ionic balance error was considered to be within the acceptable limit of $\pm 5\%$.

Water quality index and entropy weight method

To compute the WQI based on entropy weight, three steps have been followed (Adimalla et al. 2020; Maskooni et al. 2020). In the first step, entropy weight is assigned to each parameter. Entropy weight can be calculated by constructing a matrix. Considering that m ($i = 1, 2, \dots, m$) samples were monitored for water quality, with n parameters ($j = 1, 2, \dots, n$) being analyzed for each sample, then, x_{ij} represents the measured index value of parameter j in sample i . Matrix X is subsequently prepared as follows:

$$X = \begin{bmatrix} x_{11} & x_{12} & \dots & x_{1n} \\ x_{21} & x_{22} & \dots & x_{2n} \\ \vdots & \vdots & \ddots & \vdots \\ x_{m1} & x_{m2} & \dots & x_{mn} \end{bmatrix} \tag{1}$$

Owing to different units of different parameters and quantity grades, matrix X is normalized as matrix R (r_{ij}). The ratio of the index value of parameter j in sample i is calculated as follows:

$$f_{ij} = \frac{r_{ij}}{\sum_{i=1}^m r_{ij}} \tag{2}$$

The information entropy of parameter j is expressed as follows:

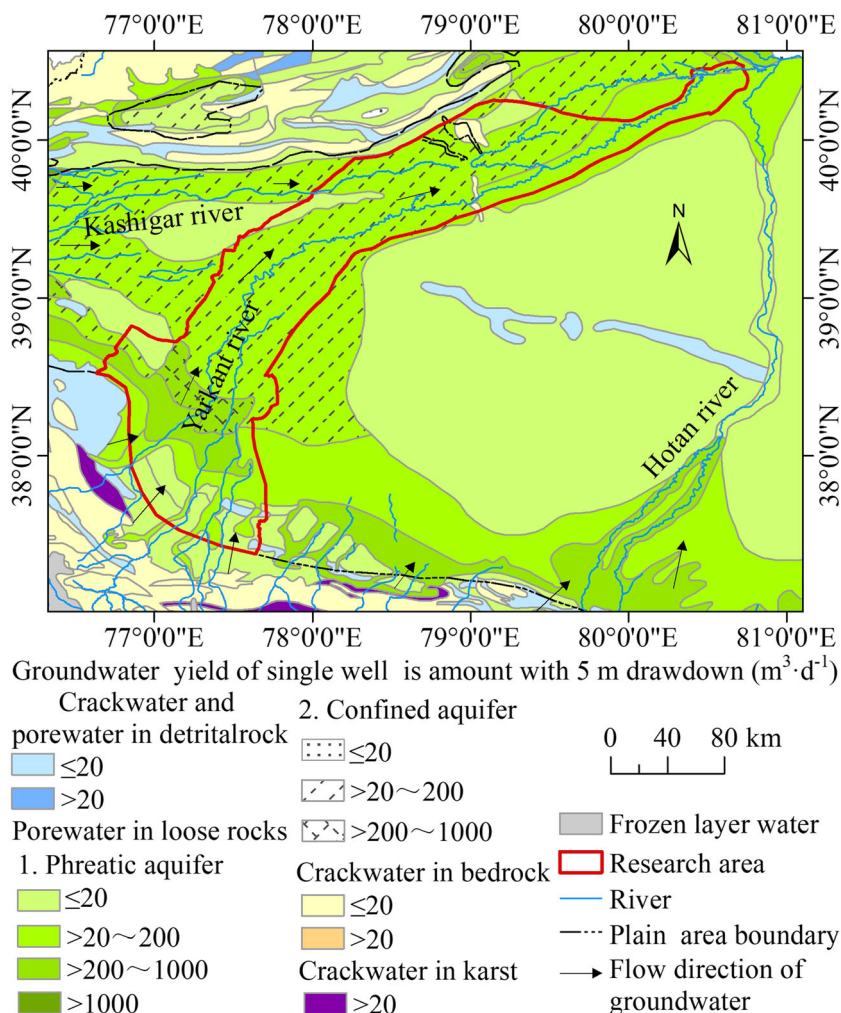
$$h_j = -\frac{1}{\ln m} \sum_{i=1}^m f_{ij} \ln f_{ij} \tag{3}$$

where h_j is the entropy value of parameter j . The entropy weight of each parameter can then be calculated as follows:

$$w_j = \frac{1-h_j}{n-\sum_{j=1}^n h_j} \tag{4}$$

where w_j is the entropy weight of parameter j .

Fig. 2 Regional hydrogeological map of the plain area in the Yarkant River Basin



In the second step, a quality rating scale (q_{ij}) is assigned for each parameter as follows:

$$q_{ij} = \frac{x_{ij}}{s_j} \times 100 \tag{5}$$

where S_j is the standard value of parameter j as per the WHO (2011) guideline (Table 1).

In the third step, the WQI of sample i is calculated as follows:

$$WQI_i = \sum_{j=1}^n w_j \times q_{ij} \tag{6}$$

The WQI values can be categorized into five classes (Alghamdi et al. 2020), as shown in Table 2.

Geostatistical analysis

The semivariogram models and ordinary kriging are applied for spatial distribution of groundwater quality parameter by ArcGIS software. The semivariogram was the main tool in geostatistics that expresses spatial correlation between adjacent observations (Arslan 2012; Rakib et al. 2020).

Semivariogram model was important for structural analysis and spatial interpolation. Assuming the normality of groundwater quality variables is crucial for obtaining reliable results in parametric statistical tests (Machiwal et al. 2018). In this study, Kolmogorov-Smirnov normality test was used to examine the normal distribution of variables. Afterwards, semivariogram model was used to identify the best predictive model. The semivariogram is calculated as follows:

$$\gamma_h = \frac{1}{2n} \sum_{i=1}^n [z(x_i) - z(x_i + h)]^2 \tag{7}$$

where represents one-half of the variance of difference between spatially distributed data points separated by distance h ; $z(x_i)$ represents the value of variable at location x_i ; $z(x_i+h)$ represents the value of other points separated from x_i by distance h ; and n represents the number of sampled points used, separated by distance h .

Because of its easy calculation and prediction accuracy compared to the other kriging methods (Bhuiyan et al. 2016), ordinary kriging was considered to be an exact interpolator with minimum mean error for finding the best linear

Table 1 Statistics of hydrochemistry parameters of groundwater in single structure phreatic aquifer (SSPA), multilayered structure phreatic aquifer (MSPA), multilayered structure confined aquifer (MSCA), and all samples (All) of the Yarkant River Basin, relative weight of the parameters, and World Health Organization (WHO) water quality standards

Parameters	SSPA (N=14)			MSPA (N=38)			MSCA (N=45)			All (N=97)			WHO standards	Weight (W _j)
	Mean	Min	Max	Mean	Min	Max	Mean	Min	Max	Mean	Min	Max		
K ⁺	33.31	6.01	120.44	11.23	3.48	37.84	38.26	4.82	211.44	32.42	3.48	211.44	20	0.092
Na ⁺	467.76	29.85	1192.84	166.63	13.10	1192.84	589.74	13.45	2137.87	480.89	13.10	2137.87	200	0.080
Ca ²⁺	282.51	29.50	621.36	155.46	39.31	557.08	293.23	26.37	858.00	269.15	26.37	858.00	200	0.056
Mg ²⁺	144.58	27.23	353.78	59.47	17.30	114.24	159.09	34.66	435.00	139.03	17.30	435.00	150	0.048
Cl ⁻	530.70	69.38	1379.28	252.19	51.60	1548.64	771.95	46.84	3102.50	602.42	46.84	3102.50	250	0.090
SO ₄ ²⁻	1187.39	167.96	2709.82	444.17	156.81	1795.90	1282.35	131.44	4050.00	1124.17	131.44	4050.00	250	0.068
HCO ₃ ⁻	376.86	128.59	766.42	220.00	90.56	400.69	301.81	53.13	550.06	319.40	53.13	766.42	120	0.023
NO ₃ ⁻	4.87	0.05	53.24	8.78	0.08	42.60	2.54	0.05	49.30	4.35	0.05	53.24	20	0.235
F ⁻	1.06	0.40	4.62	0.55	0.23	1.26	0.70	0.06	2.01	0.82	0.06	4.62	1.5	0.045
pH	7.34	6.48	7.78	7.97	7.35	8.50	7.70	6.85	8.60	7.60	6.48	8.60	6.5–8.5	0.017
TDS	2888.84	604.00	6396.01	1264.39	468.00	5674.00	3249.87	468.00	9250.00	2821.87	468.00	9250.00	1000	0.068
TH	1300.71	322.22	2992.99	632.95	328.00	1861.71	1419.76	314.85	3840.00	1259.56	314.85	3840.00	500	0.069
DO	2.66	0.61	10.85	0.92	0.60	2.27	2.29	0.60	8.91	2.24	0.60	10.85	3	0.109

N is groundwater sample number, pH is dimensionless, the other parameters are mg·L⁻¹

unbiased estimate. Interpolation acceptability criteria to ensure unbiased estimates were evaluated by cross-validation. The mean standardized error (MSE) and root mean square standardized error (RMSSE) values of the model approach to 0 and 1 respectively, which indicates that the model performance is fit (Kaur and Rishi 2018).

Hydrogeochemistry

Saturation index (SI) can be used to identify the geochemical reactions that control water-rock interaction (Ferchichi et al. 2017). SI was calculated as follows:

$$SI = \log\left(\frac{IAP}{KT}\right) \tag{8}$$

where IAP represents the ionic activity product of the water samples and KT represents the equilibrium constant at the sample temperature. SI = 0 denotes the solubility equilibrium of mineral phase in the groundwater, SI < 0 indicates the undersaturation of groundwater with this mineral, and SI > 0

indicates the supersaturated of groundwater with the mineral and its inability to dissolve other minerals (Bouderbala and Gharbi 2017).

Sodium adsorption ratio (SAR) can reflect the cation exchange between Na⁺ in groundwater and Ca²⁺ and Mg²⁺ in aquifers (Ferchichi et al. 2017). The larger the SAR, the more obvious the cation exchange. SAR was calculated as follows:

$$SAR = \frac{K^+ + Na^+}{\sqrt{\frac{Mg^{2+} + Ca^{2+}}{2}}} \tag{9}$$

where Na⁺, K⁺, Ca²⁺, and Mg²⁺ are in meq·L⁻¹.

Descriptive statistical analysis (range, median and mean) and comparison with WHO standard of measured values were done by using Excel. The PHREEQC was used for calculating SI. The ion ratio diagram was drawn by Origin software. The data of land use in 2018 was obtained from the Data Center of Resources and Environmental Sciences, Chinese Academy of Sciences (<http://www.resdc.cn>), and the described in detail were shown in Ning et al. (2018).

Results and discussions

Hydrochemical characteristics of groundwater

Detailed statistics of hydrochemical parameters of the groundwater in the plain area of the Yarkant River Basin are shown in Table 1. The pH of the groundwater was slightly alkaline to neutral, ranging from 6.48 to 8.60 with a mean value of 7.60 in

Table 2 Water quality index (WQI) classification

Range	Water quality type
< 50	Excellent
50–100	Good
100–200	Medium
200–300	Poor
> 300	Extremely poor

all groundwater samples (All). TDS in All varied from 468.00 to 9250.00 mg·L⁻¹, with a mean value of 2821.87 mg·L⁻¹. TH ranged from 314.85 to 3840.00 mg·L⁻¹, with a mean value of 1259.56 mg·L⁻¹ in All. The mean values of TDS and TH shown the trend of MSCA > SSPA > MSPA. The order followed by the mean value for cation in all aquifers was Na⁺ > Ca²⁺ > Mg²⁺ > K⁺ and for anions was SO₄²⁻ > Cl⁻ > HCO₃⁻ > NO₃⁻ > F⁻. Variances were observed in the groundwater chemistry types in different aquifers. Piper trilinear diagram (Fig. 3) shows that the dominant water types were SO₄·HCO₃-Ca·Na, SO₄·HCO₃-Ca·Mg, and SO₄·Cl-Na·Ca in SSPA, SO₄·Cl-Na·Mg, SO₄·Cl·HCO₃-Na·Ca, and SO₄·HCO₃·Cl-Ca·Na in MSPA, and of SO₄·Cl-Na·Ca, Cl·SO₄-Na·Ca, and HCO₃·SO₄-Mg·Ca in MSCA.

Table 3 shows the number and proportion of parameters greater than the acceptable values for drinking water as per WHO standards. The largest exceedance was observed for HCO₃⁻ in SSPA (85.71%), followed by TH and SO₄²⁻ (57.14% proportion for both), while Mg²⁺, F⁻, pH, and DO were not found to exceed the limit. The largest exceedance was observed for HCO₃⁻ (100.00%) in MSPA, followed by SO₄²⁻ (94.74%). The smallest exceedance rate was observed for pH (2.63%). Furthermore, the largest exceedance was observed for HCO₃⁻ (95.11%) in MSCA, followed by SO₄²⁻ (91.11%), with pH and NO₃⁻ exhibiting the smallest exceedances (2.22%). The main parameter exceeding the acceptable value of drinking water in WHO standard were HCO₃⁻, SO₄²⁻, TH, TDS, and Cl⁻ (Table 3). Luan et al. (2017) showed that the groundwater parameters exceeding the acceptable value of the standards for drinking water quality of China were TH, TDS, Cl⁻, and SO₄²⁻ in rural areas of

Table 3 Number and rate of exceeding standard in single structure phreatic aquifer (SSPA), multilayered structure phreatic aquifer (MSPA), and multilayered structure confined aquifer (MSCA)

Parameters	SSPA		MSPA		MSCA	
	Number	Rate/%	Number	Rate/%	Number	Rate/%
K ⁺	1	7.14	19	50.00	25	55.56
Na ⁺	2	14.29	27	71.05	30	66.67
Ca ²⁺	1	7.14	22	57.89	22	48.89
Mg ²⁺	0	0.00	15	39.47	21	46.67
Cl ⁻	3	21.43	27	71.05	34	75.56
SO ₄ ²⁻	8	57.14	36	94.74	41	91.11
HCO ₃ ⁻	12	85.71	38	100.00	43	95.56
NO ₃ ⁻	2	14.29	4	10.53	1	2.22
F ⁻	0	0.00	7	18.42	3	6.67
pH	0	0.00	1	2.63	1	2.22
TDS	6	42.86	35	92.11	38	84.44
TH	8	57.14	34	89.47	38	84.44
DO	0	0.00	9	23.68	14	31.11

Yarkant River Basin. Different from this study, HCO₃⁻ and cation (K⁺, Mg²⁺, Na⁺ and Ca²⁺) were not considered in Luan et al. (2017) according to the standards for drinking water quality of China.

Groundwater quality assessment

Entropy weight does not rely on subjective judgement for assigning weights, which can improve the WQI. The physico-chemical parameters with the highest entropy weight have the greatest impact on overall groundwater quality (Islam et al. 2017a). The entropy weights of NO₃⁻ was the largest, which had the highest effect on overall groundwater quality of the study area (Table 1). The effects of other parameters on overall groundwater quality decreased in the following order: DO > K⁺ > Cl⁻ > Na⁺ > TH > TDS > SO₄²⁻ > Ca²⁺ > Mg²⁺ > F⁻ > HCO₃⁻ > pH. The pH has a minimal impact on overall groundwater quality of the study region. The calculation results indicated that the ranges of WQI of all samples was 31.79 to 549.37 with an average of 158.50. The groundwater quality varied from excellent to extremely poor. In total, 31 samples were classified as good quality, constituting the largest proportion (31.96%) (Fig. 4), and 22 (22.68%), 18 (18.56%) and 14 (14.43%) samples were classified as poor, medium and excellent quality, respectively. Extremely poor quality constituted the least proportion of 12.37% (12 samples) in All. The ranges of WQI of SSPA were 31.79 to 291.43, with an average of 89.74. Excellent quality constituted the largest proportion (50.00%) in SSPA, followed by good quality (35.72%). The WQI of MSPA ranged from 36.69 to

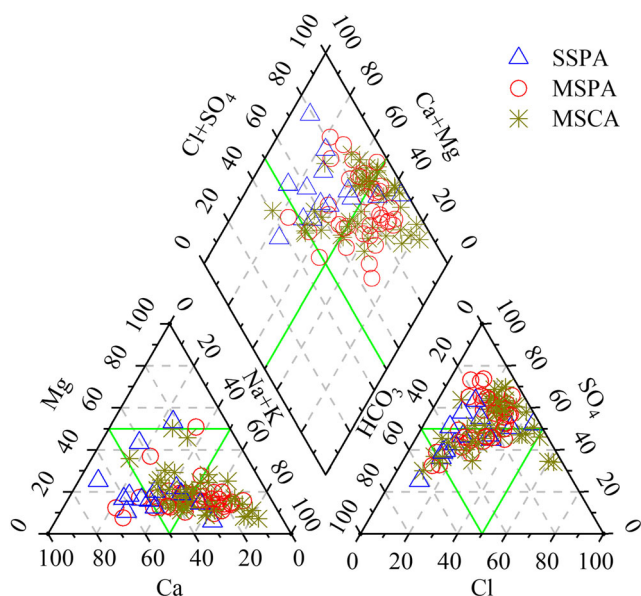
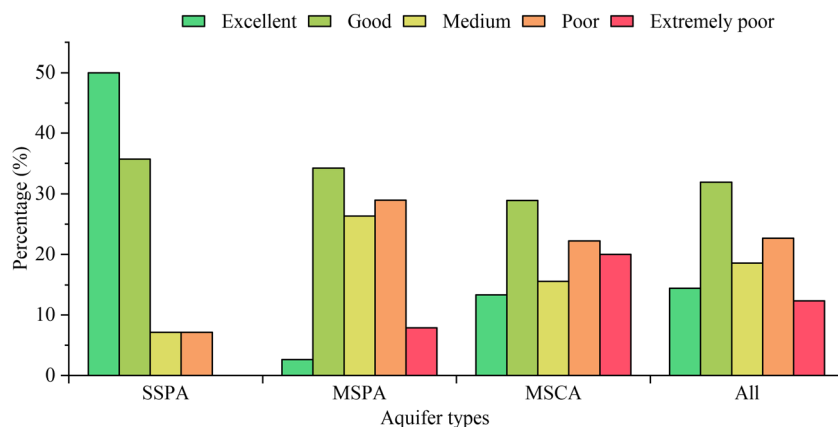


Fig. 3 Piper trilinear diagram in single structure phreatic aquifer (SSPA), multilayered structure phreatic aquifer (MSPA), and multilayered structure confined aquifer (MSCA)

Fig. 4 Proportion of different levels of groundwater quality in single structure phreatic aquifer (SSPA), multilayered structure phreatic aquifer (MSPA), multilayered structure confined aquifer (MSCA), and all samples (All)



321.17, with an average of 163.01. The proportion of good water in MSPA was the highest (34.21%), followed by poor quality (28.95%). The ranges of WQI of MSCA was 36.63 to 549.37, with an average of 179.83. Good quality constituted the highest proportion in MSCA (28.89%), with a non-negligible proportion (20.00%) of extremely poor quality.

The WQI values of phreatic aquifer (PA, including SSPA and MSPA) and MSCA followed normal distribution after logarithmic-transformation by the Kolmogorov-Smirnov test. Exponential and Gaussian models were applied for the WQI of PA and MSCA, respectively. The nugget, sill, and the range values of the model are shown in Table 4. The R^2 of the model was 0.737 and 0.791 (approximately 1) for PA and MSCA, and RSS was 0.002 and 0.005 (approximately 0), respectively. The results indicated that the fit semivariogram represents very well the spatial structure of these variables in the groundwater. According to nugget to sill ratio, the spatial dependence of groundwater quality parameters can be classified as strong spatial dependence with ratio less than 0.25, moderate spatial dependence with the ratio of 0.25 to 0.75, and weak spatial dependence with the ratio of more than 0.75 (Arslan 2012; Islam et al. 2017b). Nugget to sill ratio of the WQI values in PA and MSCA were 0.078 and 0.198, respectively, which indicated strong spatial dependence (Table 4), which might be due to the low-flow conditions in major rivers, prevailing aquifer geology, and long-term geogenic processes, such as groundwater source rock, rainfall, and infiltration processes.

During cross-validation of ordinary kriging interpolation, the MSE was found to be -0.062 and -0.053 , and RMSSE was found to be 1.098 and 1.054 in the PA and MSCA,

respectively, indicating the accuracy of predictions. The spatial distribution of WQI in southern of PA was mainly good and excellent water, and medium water in the north was the largest, followed by poor water (Fig. 5a). As groundwater flows from the relatively high south areas toward the north direction, the quality of groundwater degraded from south to north in the PA. The distribution of WQI exhibited excellent, good, and an alternation of medium and poor quality (including extremely poor quality) from south to north in the MSCA (Fig. 5b). The MSCA towards north was limited by the surface water supply, slow groundwater runoff, and strong evaporation and concentration, which resulted in a larger WQI. The relatively lower WQI in the southern part of the MSCA was related to its recharge by the PA. The spatial distribution characteristics of WQI in PA and MSCA were consistent with those of Cl^- , SO_4^{2-} and TDS (Zhang et al. 2019).

Evolution process of groundwater quality

Pearson correlation analysis of 13 hydrochemical parameters was used to explain the influencing factors of groundwater quality. The absolute values of correlation coefficient were 0.30–0.50, 0.50–0.75, and > 0.75 which denoted weak, moderate, strong correlation, respectively (Islam et al. 2017a). A positive significant correlation indicated the same source, either natural or anthropogenic sources. The correlation coefficient was found to be the highest between Cl^- and Na^+ , and a highly positive correlation was observed between SO_4^{2-} and Mg^{2+} , Ca^{2+} , and Na^+ (Fig. 6), indicating that Na^+ , Ca^{2+} , Mg^{2+} , Cl^- , and SO_4^{2-} may have common sources. The pH exhibited

Table 4 Semi-variation of water quality index (WQI) of phreatic aquifer (PA, including single structure phreatic aquifer, SSPA and multilayered structure phreatic aquifer, MSPA) and multilayered structure confined aquifer (MSCA)

Type	Model	Nugget (C_0)	Sill (C_0+C)	$C_0/(C_0+C)$	Range(A_0)/km	R^2	RSS
PA	Exponential	0.007	0.090	0.078	42.157	0.737	0.002
MSCA	Gaussian	0.026	0.131	0.198	64.345	0.791	0.005

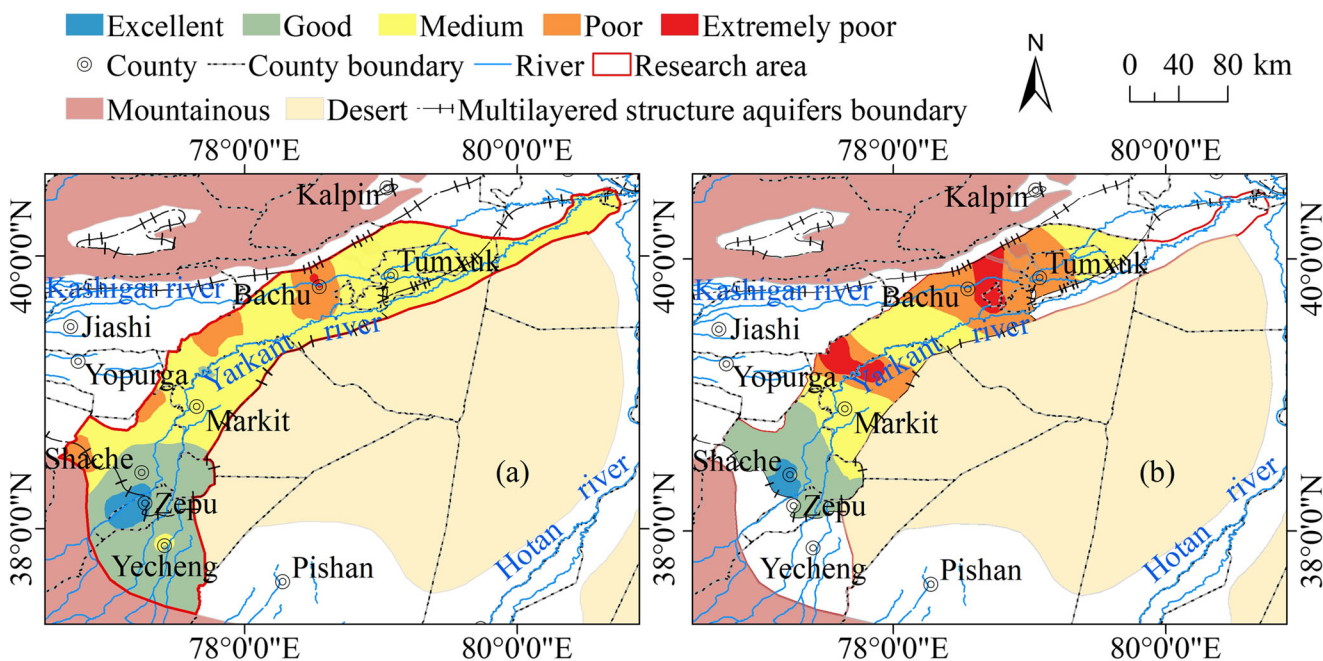


Fig. 5 Spatial distribution of water quality index (WQI) in **a** phreatic aquifer (including single structure phreatic aquifer, SSPA and multilayered structure phreatic aquifer, MSPA) and **b** multilayered structure confined aquifer (MSCA)

a negative correlation with HCO_3^- and F^- , indicating the favorability of acid environment for HCO_3^- and F^- enrichment. No obvious correlation was observed between the chemical constituents mentioned above and NO_3^- , indicating that NO_3^- may have originated from anthropogenic activities.

With the extension of the river, the groundwater quality of PA within 10 km of the river gradually degenerated from excellent quality to good, medium, and poor quality (Fig. 7). The further away from the river, the groundwater quality of SSPA gradually degenerated from excellent quality to good and poor quality on western bank of the river and from

Fig. 6 Correlation coefficients of parameters of the shallow groundwater

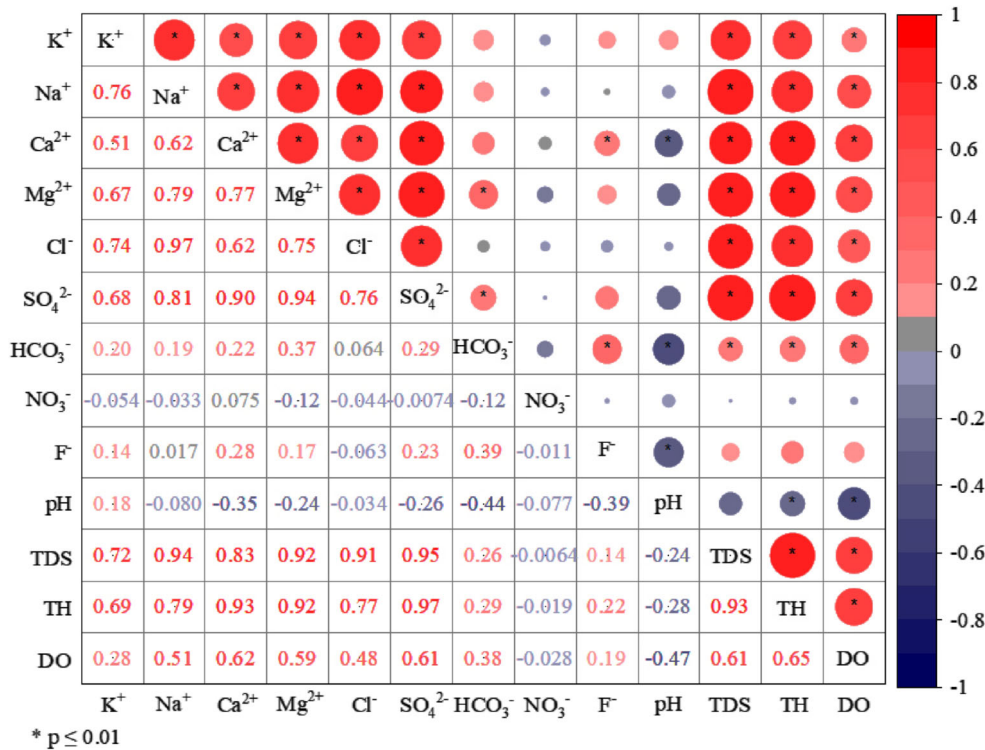
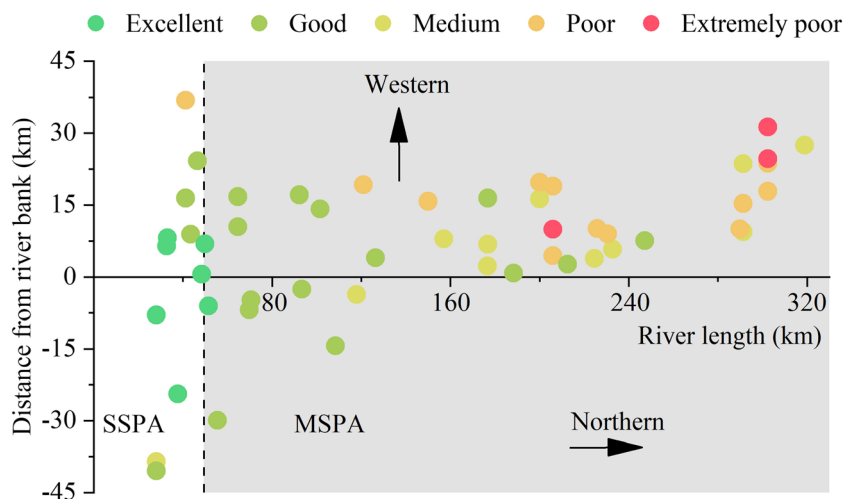


Fig. 7 The groundwater quality of phreatic aquifer (including single structure phreatic aquifer, SSPA and multilayered structure phreatic aquifer, MSPA) along the Yarkant River



excellent quality to good and medium quality on eastern. The groundwater quality of MSPA on western bank of the river gradually degenerated from good quality to poor quality at 120 km and from poor quality to extremely poor quality at 300 km. The WQI value in the south of PA was relatively small, especially SSPA, which might be related to the rapid flow of groundwater and the recharge of surface water with low concentration (Wu et al. 2008). The slow flow of groundwater in the northern low plain might increase the residence time of rock-water interactions and also increase the

concentrations of groundwater ions (Kang et al. 2016). In addition to the hydraulic connection with SSPA in the south, the surface water supply to MSCA was limited. As the MSCA was situated in a more closed environment with longer durations of water rock action, the WQI in MSCA was found to be mostly higher than that in PA.

In aquifers, the dissolution process of soluble mineral is main natural contributor to groundwater chemical composition (Abu-Alnaeem et al. 2018). The relationship between SI and WQI is shown in Fig. 8. The SI of dolomite and calcite were observed to

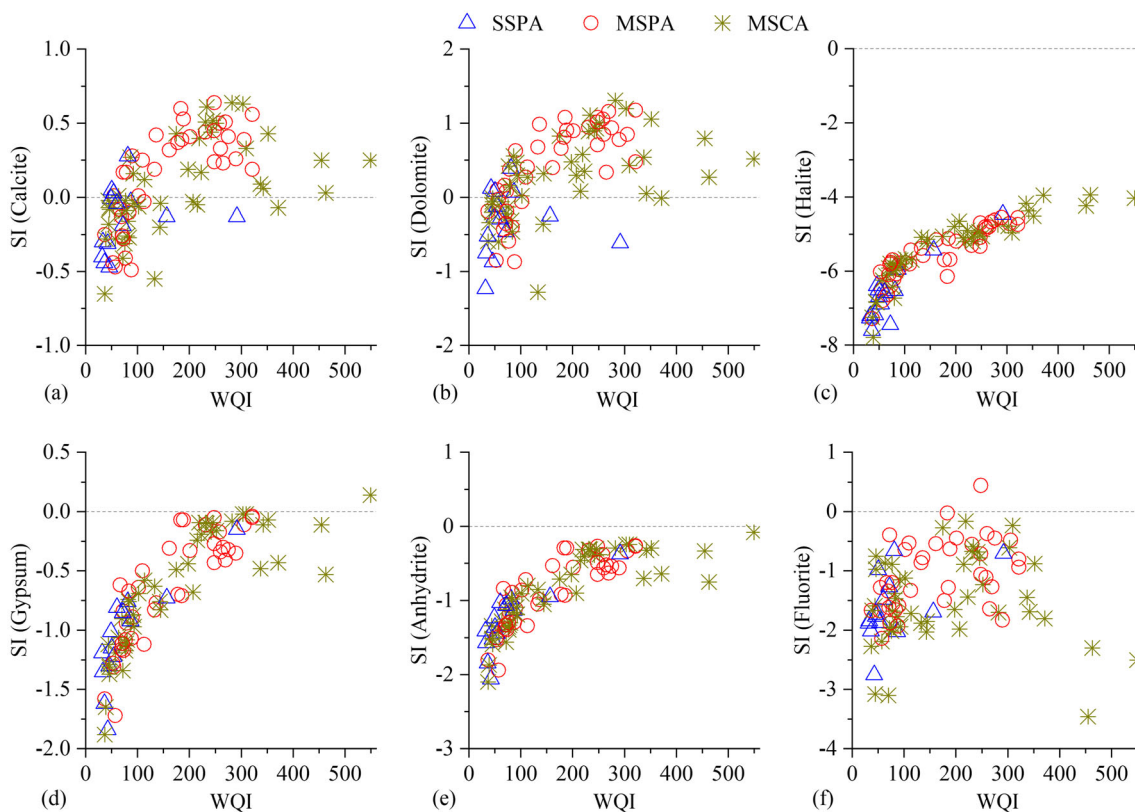


Fig. 8 Saturation index of calcite (a), dolomite (b), halite (c), gypsum (d), anhydrite (e), and fluorite (f) minerals

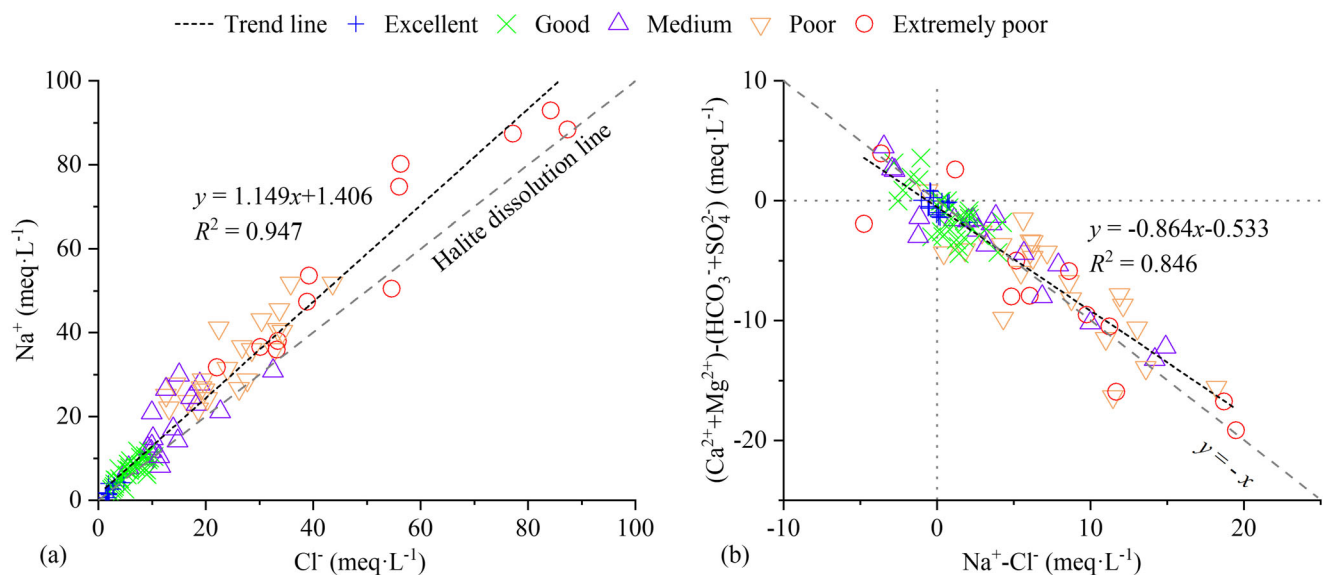


Fig. 9 Biplot of **a** Na^+ versus Cl^- and **b** $(\text{Ca}^{2+} + \text{Mg}^{2+}) - (\text{HCO}_3^- + \text{SO}_4^{2-})$ versus $\text{Na}^+ + \text{K}^+ - \text{Cl}^-$ in the hydrochemistry of the study area

be less than zero for excellent and good quality, indicating that the mineral dissolution of dolomite and calcite was the main hydrochemical process (Fig. 8a and b). In the medium, poor, and excellently poor quality, the SI of dolomite and calcite were greater than zero, indicating that dolomite and calcite had reached a saturated state, with a weak mineral dissolution. Therefore, the weak dissolution of calcite or dolomite could have likely occurred, which could be an important factor to control Ca^{2+} and Mg^{2+} concentrations in the groundwater with high WQI value. Furthermore, the concentration of Ca^{2+} (mean $269.15 \text{ mg}\cdot\text{L}^{-1}$) exceeds that of Mg^{2+} (mean $139.03 \text{ mg}\cdot\text{L}^{-1}$), indicating that the dissolution of calcite may be a dominant factor governing the groundwater chemistry (Islam et al. 2017a). The SI of halite, gypsum, anhydrite, and fluorite were less than zero and increased

with increasing WQI (Fig. 8c, d, e, and f), indicating that Na^+ , Cl^- , SO_4^{2-} , and F^- concentrations might have been controlled by the dissolution of evaporite minerals, such as halite, gypsum, and anhydrite.

Relationship between specific ions can indicate the main hydrochemical processes in groundwater. Most medium, poor, and extremely poor quality were located above the congruent dissolution line of salt rock (Fig. 9a), indicating that halite dissolution did not contribute to the dominance of Na^+ over Cl^- in the plot (El Alfy et al. 2018). Na^+ might have come from cation exchange in addition to the dissolution of salt rock. Samples with end-members 0 ($k = -1$) in the scatter plot of $(\text{Ca}^{2+} + \text{Mg}^{2+}) - (\text{HCO}_3^- + \text{SO}_4^{2-})$ versus $\text{Na}^+ + \text{K}^+ - \text{Cl}^-$ represent ions originating from mineral dissolution (Argamasilla et al. 2017; Chegbeleh et al. 2020; Saha et al. 2020). The samples were plotted away from end-members 0, indicating that Ca^{2+} and/or Mg^{2+} were derived from processes not related with carbonate or gypsum dissolution (Fig. 9b). A plot with these two indexes was enriched in $\text{Na}^+ + \text{K}^+ - \text{Cl}^-$, while $(\text{Ca}^{2+} + \text{Mg}^{2+}) - (\text{HCO}_3^- + \text{SO}_4^{2-})$ was observed to decrease, with a significantly deviating slope from mineral congruent dissolution line ($y = -x$), confirming the likelihood of ion exchange domination between Ca^{2+} , Mg^{2+} , and Na^+ in the groundwater system.

The SAR of the all groundwater ranged from 0.29 to 23.91, with an average value of 5.27. Figure 10 shows that the SAR was positively correlated with WQI ($R^2 = 0.703$), implying that the higher the WQI, the greater its SAR value and the more obvious the ion exchange effect. Most groundwater samples in the poor (95.83%) and extremely poor quality (100.00%) were located in MSPA or MSCA. The slow groundwater runoff, long water-rock interaction time, and fine sediment particles in the confined aquifer more obviously alternated the adsorption between Na^+ , Ca^{2+} , and Mg^{2+} . Ca^{2+} in the groundwater replaced a part of Na^+ adsorbed in the water-bearing medium, thus increasing Na^+ in

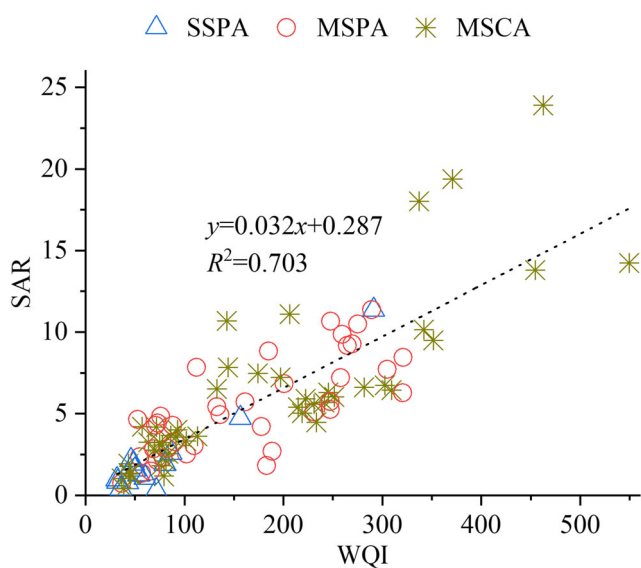


Fig. 10 Relationship between sodium adsorption ratio (SAR) and water quality index (WQI)

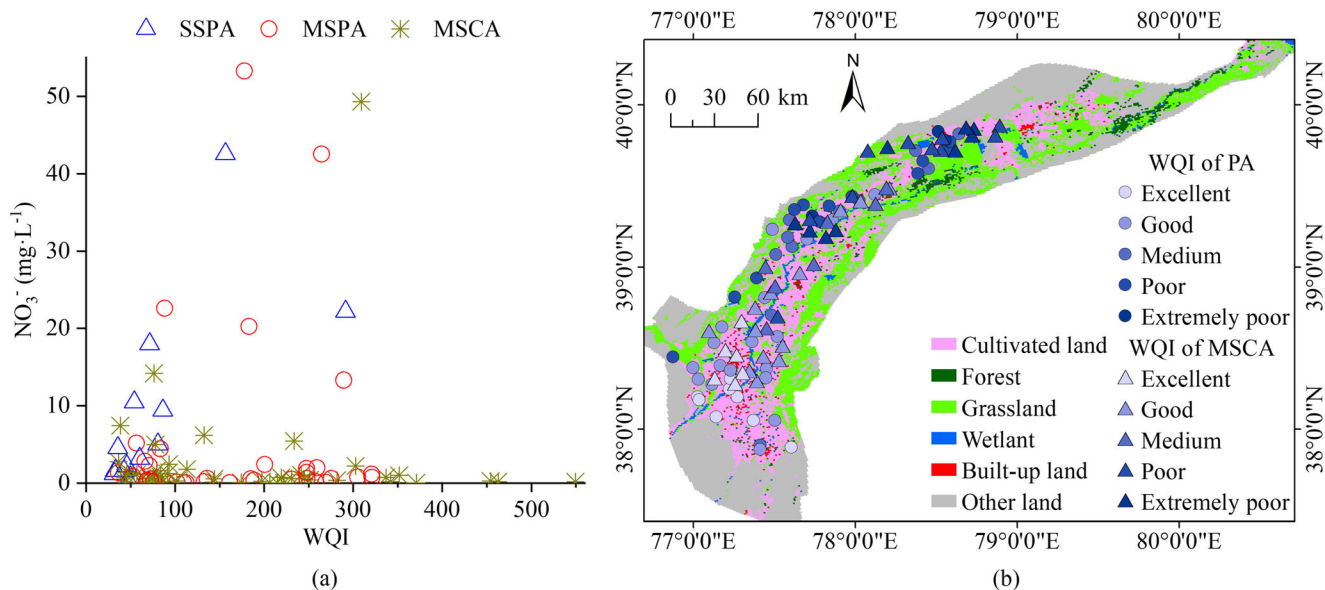


Fig. 11 **a** Relationship between NO_3^- and water quality index (WQI) and **b** the distribution of groundwater quality in land use types

groundwater and deteriorating the groundwater quality, which were the same as the groundwater in the Tarim River Basin (Xiao et al. 2014).

Natural processes play a dominant role in deteriorating groundwater quality, and the impact of human activities cannot be ignored. In recent decades, the increase of population and agricultural production had aggravated the environmental and water quality degradation of the region (Xiao et al. 2014). NO_3^- in some samples exceeded the standard value and their WQIs were found to be medium, poor, or extremely poor quality (Fig. 11a). The mean NO_3^- concentrations in SSPA and MSPA were higher than those in MSCA (Table 1), indicating the susceptibility of SSPA and MSPA to be anthropogenically contaminated. Poor and extremely poor groundwater quality were mainly located in the central and northern cultivated and built-up land (Fig. 11b). Fertilizer infiltration with irrigation water, untreated domestic sewage, and industrial effluents pollute groundwater along the groundwater channels, thus deteriorating groundwater quality (Zhang et al. 2016). As SSPA and MSPA is situated closer to the surface, it is more directly affected by man-made pollution than the MSCA. Although anthropogenic contamination has less impact on MSCA, some abandoned wells have damaged the aquifers, and contaminated of MSPA along the walls can deteriorate confined aquifer (Lin et al. 2017).

Conclusions

Groundwater was found to be slightly alkaline with high TDS and TH in the plain area of the Yarkant River Basin.

The dominant water types were found to be $\text{SO}_4\cdot\text{HCO}_3\text{-Ca}\cdot\text{Na}$, $\text{SO}_4\cdot\text{HCO}_3\text{-Ca}\cdot\text{Mg}$, and $\text{SO}_4\cdot\text{Cl}\cdot\text{Na}\cdot\text{Ca}$ in SSPA, $\text{SO}_4\cdot\text{Cl}\cdot\text{Na}\cdot\text{Mg}$, $\text{SO}_4\cdot\text{Cl}\cdot\text{HCO}_3\text{-Na}\cdot\text{Ca}$, and $\text{SO}_4\cdot\text{HCO}_3\cdot\text{Cl}\cdot\text{Ca}\cdot\text{Na}$ in MSPA, and $\text{SO}_4\cdot\text{Cl}\cdot\text{Na}\cdot\text{Ca}$, $\text{Cl}\cdot\text{SO}_4\cdot\text{Na}\cdot\text{Ca}$, and $\text{HCO}_3\cdot\text{SO}_4\cdot\text{Mg}\cdot\text{Ca}$ in MSCA. In all, the proportion that concentration of HCO_3^- more than the standard values for drinking water as per the WHO guidelines was largest, followed by SO_4^{2-} . Comprehensive evaluation value (WQI) (ranged between 31.79 and 549.37, with an average of 158.50) indicated that the groundwater quality varied from excellent to extremely poor. The largest proportion was of good quality (31.96%), followed by poor quality (22.68%). The proportions of medium, excellent, and extremely poor quality were 18.56%, 14.43%, and 12.37%, respectively. Nugget to sill ratio of the WQI values in PA (including SSPA and MSPA) and MSCA were 0.078 and 0.198, respectively, which indicated strong spatial dependence. The slow groundwater runoff, long water-rock interaction time, and fine sediment particles, the groundwater quality degraded from south to north in PA and MSCA. The deterioration of water quality may be controlled by the dissolution of evaporite minerals, such as halite, gypsum, and anhydrite and ion exchange process. In addition, the local effects of anthropogenic pollution on groundwater quality cannot be ignored. For sustainable development, the monitoring and management of groundwater quality for drinking and irrigation was needed in this area. The scale of groundwater exploitation should be controlled and the permission system of groundwater intake should be strictly implemented. The poor quality or abandoned wells should be treated in time by means of sealing, cementing, and backfilling to prevent the groundwater quality of MSPA from the MSCA.

Declarations**Ethics approval** Not applicable**Consent to participate** Not applicable**Consent for publication** Not applicable**Conflict of interest** The authors declare that they have no conflict of interest.

Author contribution Jie Zhang: investigation, writing-original draft, writing-review and editing, and supervision. Jinlong Zhou: data curation, methodology, resources, writing-review and editing. Yin Zhu Zhou: methodology, writing-review, editing and formal analysis. Yanyan Zeng: writing-review, editing, formal analysis and software. Yuanyuan Ji: writing-review and editing and software. Ying Sun: investigation and software. Mi Lei: investigation and software. All authors read and approved the final manuscript.

Funding This work was financially supported by the National Natural Science Foundation of China [No. 41662016], the University Research Project of Xinjiang Uygur Autonomous Region [No. XJEDU2018Y020], and the Water Conservancy Engineering Key Discipline Project of Xinjiang Agricultural University [No. SLXK2019-10].

Data availability Not applicable**References**

- Abu-Alnaeem MF, Yusoff I, Ng TF, Alias Y, Raksmeay M (2018) Assessment of groundwater salinity and quality in Gaza coastal aquifer, Gaza Strip, Palestine: An integrated statistical, geostatistical and hydrogeochemical approaches study. *Sci Total Environ* 615: 972–989. <https://doi.org/10.1016/j.scitotenv.2017.09.320>
- Adimalla N, Qian H, Li P (2020) Entropy water quality index and probabilistic health risk assessment from geochemistry of groundwaters in hard rock terrain of Nanganur County, South India. *Geochemistry* 80(4):125544. <https://doi.org/10.1016/j.chemer.2019.125544>
- Alghamdi AG, Aly AA, Aldhumri SA, Al-Barakaha FN (2020) Hydrochemical and quality assessment of groundwater resources in Al-Madinah City, Western Saudi Arabia. *Sustainability* 12: 3106. <https://doi.org/10.3390/su12083106>
- Ali M, Moheghy MA, Moheghi MM, Mehiqi M, Zandvakili Z (2020) Environmental hydrogeochemistry characteristics, controlling factors and groundwater quality assessment in Herat City, West Afghanistan. *Water Res* 47:325–335. <https://doi.org/10.1134/S0097807820020104>
- Argamasilla M, Barbera JA, Andreo B (2017) Factors controlling groundwater salinization and hydrogeochemical processes in coastal aquifers from southern Spain. *Sci Total Environ* 580:50–68. <https://doi.org/10.1016/j.scitotenv.2016.11.173>
- Arslan H (2012) Spatial and temporal mapping of groundwater salinity using ordinary kriging and indicator kriging: the case of Bafra Plain, Turkey. *Agric Water Manag* 113:57–63. <https://doi.org/10.1016/j.agwat.2012.06.015>
- Bhakar P, Singh AP (2018) Groundwater quality assessment in a hyper-arid region of Rajasthan, India. *Nat Resour Res* 28:505–522. <https://doi.org/10.1007/s11053-018-9405-4>
- Bhuiyan MAH, Bodrud-Doza M, Islam ARMT, Rakib MA, Rahman MS, Ramanathan AL (2016) Assessment of groundwater quality of Lakshimpur district of Bangladesh using water quality indices, geostatistical methods, and multivariate analysis. *Environ Earth Sci* 75:1020. <https://doi.org/10.1007/s12665-016-5823-y>
- Bouderbala A, Gharbi BY (2017) Hydrogeochemical characterization and groundwater quality assessment in the intensive agricultural zone of the Upper Cheliff plain, Algeria. *Environ Earth Sci* 76: 744. <https://doi.org/10.1007/s12665-017-7067-x>
- Boutera O, Mebarki A, Bouaicha F, Nouaceur Z, Laignel B (2019) Groundwater quality assessment using multivariate analysis, geostatistical modeling, and water quality index (WQI): a case of study in the Boumerzoug-El Khroub valley of Northeast Algeria. *Acta Geochim* 38:796–814. <https://doi.org/10.1007/s11631-019-00329-x>
- Bouzourra H, Bouhlila R, Elango L, Slama F, Ouslati N (2015) Characterization of mechanisms and processes of groundwater salinization in irrigated coastal area using statistics, GIS, and hydrogeochemical investigations. *Environ Sci Pollut Res* 22:2643–2660. <https://doi.org/10.1007/s11356-014-3428-0>
- Chang J, Kan Y, Wang Y, Huang Q, Chen L (2016) Conjunctive operation of reservoirs and ponds using a simulation-optimization model of irrigation systems. *Water Resour Manag* 31:995–1012. <https://doi.org/10.1007/s11269-016-1559-4>
- Chegbeleh LP, Akurugu BA, Yidana SM (2020) Assessment of groundwater quality in the Talensi District, Northern Ghana. *Sci World J* 2020:8450860–8450824. <https://doi.org/10.1155/2020/8450860>
- Dehbandi R, Moore F, Keshavarzi B (2018) Geochemical sources, hydrogeochemical behavior, and health risk assessment of fluoride in an endemic fluorosis area, central Iran. *Chemosphere* 193:763–776. <https://doi.org/10.1016/j.chemosphere.2017.11.021>
- Egbi CD, Anornu G, Appiah-Adjei EK, Ganyaglo SY, Dampare SB (2018) Evaluation of water quality using hydrochemistry, stable isotopes, and water quality indices in the Lower Volta River Basin of Ghana. *Environ Dev Sustain* 21:3033–3063. <https://doi.org/10.1007/s10668-018-0180-5>
- El Alfy M, Alharbi T, Mansour B (2018) Integrating geochemical investigations and geospatial assessment to understand the evolutionary process of hydrochemistry and groundwater quality in arid areas. *Environ Monit Assess* 190:277. <https://doi.org/10.1007/s10661-018-6640-4>
- Ferchichi H, Farhat B, Ben-Hamouda MF, Ben-Mammou A (2017) Understanding groundwater chemistry in Mediterranean semi-arid system using multivariate statistics techniques and GIS methods: case of Manouba aquifer (Northeastern Tunisia). *Arab J Geosci* 10:530. <https://doi.org/10.1007/s12517-017-3314-4>
- Hayat E, Baba A (2017) Quality of groundwater resources in Afghanistan. *Environ Monit Assess* 189:318. <https://doi.org/10.1007/s10661-017-6032-1>
- Huang T, Pang Z (2012) The role of deuterium excess in determining the water salinisation mechanism: a case study of the arid Tarim River Basin, NW China. *Appl Geochem* 27:2382–2388. <https://doi.org/10.1016/j.apgeochem.2012.08.015>
- Islam ARMT, Ahmed N, Bodrud-Doza M, Chu R (2017a) Characterizing groundwater quality ranks for drinking purposes in Sylhet district, Bangladesh, using entropy method, spatial autocorrelation index, and geostatistics. *Environ Sci Pollut Res* 24(34):26350–26374. <https://doi.org/10.1007/s11356-017-0254-1>
- Islam MA, Rahman MM, Bodrud-Doza M, Muhib MI, Shammi M, Zahid A, Akter Y, Kurasaki M (2017b) A study of groundwater irrigation water quality in south-central Bangladesh: a geo-statistical model approach using GIS and multivariate statistics. *Acta Geochim* 37: 193–214. <https://doi.org/10.1007/s11631-017-0201-3>
- Islam ARMT, Mamun AA, Rahman MM, Zahid A (2020a) Simultaneous comparison of modified-integrated water quality and entropy weighted indices: Implication for safe drinking water in the coastal region of Bangladesh. *Ecol Indic* 113:106229. <https://doi.org/10.1016/j.ecolind.2020.106229>
- Islam ARMT, Siddiqua MT, Zahid A, Tasnim SS, Rahman MM (2020b) Drinking appraisal of coastal groundwater in Bangladesh: An approach of multi-hazards towards water security and health safety.

- Chemosphere 255:126933. <https://doi.org/10.1016/j.chemosphere.2020.126933>
- Kang N, Tang H, Chen S, Feng JY (2016) Study on groundwater environmental background values in Yarkant River Basin. *Ground Water* 38:80–82 (in Chinese)
- Kaur L, Rishi MS (2018) Integrated geospatial, geostatistical, and remote-sensing approach to estimate groundwater level in North-western India. *Environ Earth Sci* 77:786. <https://doi.org/10.1007/s12665-018-7971-8>
- Keshavarzi B, Moore F, Mosaferi M, Rahmani F (2011) The source of natural arsenic contamination in groundwater, West of Iran. *Water Qual Expos Hea* 3:135–147. <https://doi.org/10.1007/s12403-011-0051-x>
- Kolsi SH, Bouri S, Hachicha W, Dhia HB (2013) Implementation and evaluation of multivariate analysis for groundwater hydrochemistry assessment in arid environments: a case study of Hajeb Elyoun-Jelma, Central Tunisia. *Environ Earth Sci* 70:2215–2224. <https://doi.org/10.1007/s12665-013-2377-0>
- Li Q, Zhou J, Zhou Y, Jia R (2013) Salinization of deep groundwater in plain areas of Xinjiang: causes and countermeasures. *Desalin Water Treat* 52:2724–2733. <https://doi.org/10.1080/19443994.2013.827775>
- Lin J, Ma R, Hu Y, Sun Z, Wang Y, McCarter CPR (2018) Groundwater sustainability and groundwater/surface-water interaction in arid Dunhuang Basin, northwest China. *Hydrogeol J* 26:1559–1572. <https://doi.org/10.1007/s10040-018-1743-0>
- Lin L, Zeng YY, Zhou JL (2017) Cause analysis of salinization of deep confined groundwater in Tarim Basin Plain. *Yellow River* 39:72–75 (in Chinese)
- Luan FJ, Zhou JL, Zeng YY, Jia RL (2017) Evaluation of groundwater quality security in rural areas of Yarkant River Basin. *Yellow River* 39:68–71 (in Chinese)
- Machiwal D, Cloutier V, Güler C, Kazakis N (2018) A review of GIS-integrated statistical techniques for groundwater quality evaluation and protection. *Environ Earth Sci* 77:681. <https://doi.org/10.1007/s12665-018-7872-x>
- Maskooni EK, Naseri-Rad M, Berndtsson R, Nakagawa K (2020) Use of heavy metal content and modified water quality index to assess groundwater quality in a semiarid area. *Water* 12:1115. <https://doi.org/10.3390/w12041115>
- Naseem S, Husain V, Bano S (2018) Origin of salinity and Other constituents in Indus Deltaic Plain groundwater, Thatta District, Pakistan. *J Coast Res* 344:883–891. <https://doi.org/10.2112/jcoastres-d-17-00052.1>
- Ning J, Liu J, Kuang W, Xu X, Zhang S, Yan C, Li R, Wu S, Hu Y, Du G, Chi W, Pan T, Ning J (2018) Spatiotemporal patterns and characteristics of land-use change in China during 2010–2015. *J Geogr Sci* 28(5):547–562. <https://doi.org/10.1007/s11442-018-1490-0>
- Pulido-Bosch A, Rigol-Sanchez JP, Vallejos A, Andreu JM, Ceron JC, Molina-Sanchez L, Sola F (2018) Impacts of agricultural irrigation on groundwater salinity. *Environ Earth Sci* 77:197. <https://doi.org/10.1007/s12665-018-7386-6>
- Rabei RE (2018) Assessment and modeling of groundwater quality using WQI and GIS in Upper Egypt area. *Environ Sci Pollut Res* 25:30808–30817. <https://doi.org/10.1007/s11356-017-8617-1>
- Rakib MA, Sasaki J, Matsuda H, Quraishi SB, Mahmud MJ, BodrudDoza M, Ullah AA, Fatema KJ, Newaz MA, Bhuiyan MAH (2020) Groundwater salinization and associated co-contamination risk increase severe drinking water vulnerabilities in the southwestern coast of Bangladesh. *Chemosphere* 246:125646. <https://doi.org/10.1016/j.chemosphere.2019.125646>
- Reyes-Toscano CA, Alfaro-Cuevas-Villanueva R, Cortés-Martínez R, Morton-Bermea O, Hernández-Álvarez E, Buenrostro-Delgado O, Ávila-Olivera JA (2020) Hydrogeochemical characteristics and assessment of drinking water quality in the Urban Area of Zamora, Mexico. *Water* 12:556. <https://doi.org/10.3390/w12020556>
- Saha N, Bodrud-doza M, Islam ARMT, Begum BA, Rahman MS (2020) Hydrogeochemical evolution of shallow and deeper aquifers in central Bangladesh: arsenic mobilization process and health risk implications from the potable use of groundwater. *Environ Earth Sci* 79:477. <https://doi.org/10.1007/s12665-020-09228-4>
- Schwarzenbach RP, Egli T, Hofstetter TB, von Gunten U, Wehrli B (2010) *Global Water Pollution and Human Health*. *Annu Rev Environ Resour* 35:109–136. <https://doi.org/10.1146/annurev-environ-100809-125342>
- Sethy SN, Syed TH, Kumar A (2017) Evaluation of groundwater quality in parts of the Southern Gangetic Plain using water quality indices. *Environ Earth Sci* 76:116. <https://doi.org/10.1007/s12665-017-6434-y>
- Singh CK, Shashtri S, Mukherjee S (2010) Integrating multivariate statistical analysis with GIS for geochemical assessment of groundwater quality in Shiwaliks of Punjab, India. *Environ Earth Sci* 62:1387–1405. <https://doi.org/10.1007/s12665-010-0625-0>
- Solangi GS, Siyal AA, Babar MM, Siyal P (2019) Application of water quality index, synthetic pollution index, and geospatial tools for the assessment of drinking water quality in the Indus Delta, Pakistan. *Environ Monit Assess* 191:731. <https://doi.org/10.1007/s10661-019-7861-x>
- Tabassum RA, Shahid M, Dumat C, Niazi NK, Khalid S, Shah NS, Imran M, Khalid S (2019) Health risk assessment of drinking arsenic-containing groundwater in Hasilpur, Pakistan: effect of sampling area, depth, and source. *Environ Sci Pollut Res* 26:20018–20029. <https://doi.org/10.1007/s11356-018-1276-z>
- WHO (ed) (2011) *Guidelines for drinking-water quality*, 4th edn. WHO, Geneva
- Wu QQ, Ren JG, Xu M (2008) Isotope features and supply sources of groundwater in the Yarkant River drainage area, Xinjiang. *Geol China* 35:331–336 (in Chinese)
- Xiao J, Jin Z, Wang J (2014) Assessment of the Hydrogeochemistry and Groundwater Quality of the Tarim River Basin in an Extreme Arid Region, NW China. *Environ Manag* 53:135–146. <https://doi.org/10.1007/s00267-013-0198-2>
- Zhang J, Zhou JL, Nai WH, Zeng YY, Chen YF, Wei X (2019) Spatial distribution and cause of salinization of shallow groundwater in plain terrain of the Yarkant River Basin, Xinjiang. *Trans CSAE* 35:126–134 (in Chinese)
- Zhang X, Qian H, Wu H, Chen J, Qiao L (2016) Multivariate analysis of confined groundwater hydrochemistry of a long-exploited sedimentary basin in northwest China. *J Chem* 2016:1–15. <https://doi.org/10.1155/2016/3812125>

Publisher's note Springer Nature remains neutral with regard to jurisdictional claims in published maps and institutional affiliations.